Trapped particle sideband studies

S. I. Tsunoda[a] and J. H. Malmberg
Department of Physics, University of California, San Diego, La Jolla, California 92093

(Received 13 February 1989; accepted 31 May 1989)

The behavior of sidebands growing in the presence of a launched large amplitude wave in a beam–plasma system is studied numerically. The large amplitude wave traps the beam and both the upper and the lower sidebands become unstable. The behavior of the instability is found to be dependent on a phase relationship that exists between the two sidebands and the large amplitude wave. The essential features of the instability are well described by a simple model in which the trapped electrons are replaced by a single particle oscillating in each well of the large amplitude wave.

I. INTRODUCTION

It is known from both experimental and theoretical work[1–8] that the nonlinear trapped particle state that results from the trapping of electrons in a single wave is unstable to the growth of sidebands. In the experiments[1–5] it was observed that in the presence of a wave at frequency f_L, whose amplitude is sufficiently large to cause trapping, waves at frequencies near $f = f_L \pm f_b$ are unstable and grow from noise. The bounce frequency associated with the nonlinear trapped particle state is $f_b = \sqrt{ek_L E/m}/2\pi$, where k_L is the wavenumber of the large amplitude wave (LAW), E is the peak electric field, $-e$ is the electric charge, and m is the electron mass.

An important simplification to the theoretical description of the sideband instability was given by Kruer, Dawson, and Sudan[6] (KDS). They modeled the trapped particle state as a single particle oscillating in a harmonic well [see Fig. 1(a)]. In the rest frame of the harmonic well, consider a sideband traveling with velocity Δv. A resonant interaction occurs when the sideband, whose wavelength is $\lambda = 2\pi/k$, travels a distance λ during a particle bounce time; that is, when $\Delta v/f_b = \lambda$. In the lab frame, if the well is traveling with velocity $v_L = 2\pi f_L/k_L$, the above resonance condition becomes

$$f = f_L(k/k_L) \pm f_b. \tag{1}$$

The plus or minus sign appears because both upper and lower sidebands can be resonant in this way; and, in fact, both upper and lower sidebands are unstable. An important feature of the KDS theory is that it fundamentally involves both upper and lower sidebands.

The growth mechanism of the instability is rather interesting and can be seen as follows. Let us assume that the particle is at the bottom of the well, and that, in the lab frame, the particle and the LAW are traveling with essentially the same velocity in the $+z$ direction. Figures 1(b) and 1(c) show the situation in the rest frame of the LAW. The waves labeled A and B are lower and upper sidebands that travel in opposite directions in the LAW rest frame. Let us suppose that at $t = 0$ the sideband phases are as shown in Fig. 1(b). Let us further suppose that there is a small velocity perturbation of the particle as shown. Since the particle is on the decelerating side of the well of sideband A, the particle gives up energy to sideband A and sideband A grows. The particle is on the accelerating side of the well of sideband B. The particle receives energy from sideband B and causes sideband B to damp. However, since the particle is traveling in the $+z$ direction, it stays on the decelerating part of sideband A (causing growth) for a relatively long time and on the accelerating part of sideband B (causing damping) for a relatively short time. When the resonance condition [Eq. (1)] is satisfied, the situation at $t = 1/(2f_b)$ is as shown in Fig. 1(c). The particle is now moving in the $-z$ direction and is now on the accelerating side (causing damping) of sideband A for a relatively short time and on the decelerating side (causing growth) of sideband B for a relatively long time. The net result is the growth of both sidebands. During the sideband growth, the sidebands exert oppositely directed forces on the particle. However, the net force is always such that it causes an increase in the oscillation amplitude of the particle. This causes the particle to spend an even longer time on the decelerating parts of the sidebands and an even

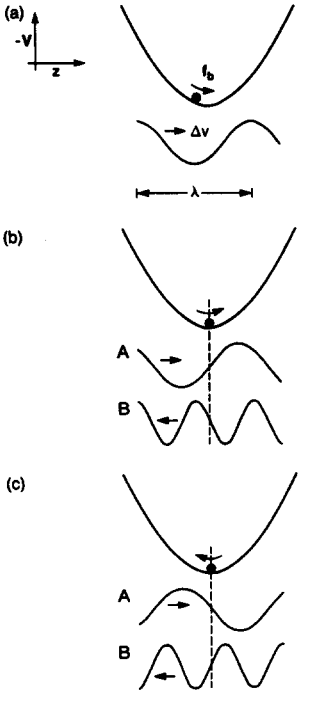

FIG. 1. Simple physical picture illustrating the sideband resonance condition and the growth mechanism.

[a] Present address: General Atomics, P.O. Box 85608, San Diego, California 92138.

 0899-8221/89/101958-06$01.90

shorter time on the accelerating parts which, in turn, causes more growth. The source of free energy for the instability is the electron kinetic energy in the lab frame. The electron oscillations have negative energy. Thus, as the instability proceeds, the electron oscillation amplitude increases, while the lab frame electron kinetic energy decreases.

Since in the KDS approximation the replacement of the trapped electrons by a single charged particle represents a highly nonlinear state of the beam, one might expect coupling between the waves, and, in particular, one might expect the sideband behavior to be sensitive to the relative phases of the waves. This is indeed the case in the initial growth region of the instability. By "initial growth region" we mean the region from the beginning of the interaction to a point several e-foldings away. Thus the physical situation addressed by the KDS model is quite different from quasilinear type interactions[4,5,8] in which wave phases are unimportant and where the growth is determined solely by the time-averaged velocity distribution function.

In the initial growth region one can represent the LAW and the small amplitude upper and lower sidebands as a mixture of an amplitude modulation and a frequency modulation of the LAW. In the limits $k/k_L \sim 1, f_b/f_L \ll 1$, and in the limit of low beam density, the KDS model predicts that the three-wave system evolves to pure amplitude modulation of the LAW. This effect can be studied more generally by following the evolution of a phase relationship (which we define later) among the three waves.

We have made a numerical study of the spatially growing sideband stability that occurs when electrons become trapped in a LAW. This study makes use of a many electron simulation and a simplified version of this simulation that is obtained by replacing the electrons with a single charged particle in each well of the LAW. This simplified situation is a generalization of the KDS model in the sense that the LAW potential well is sinusoidal rather than harmonic; the particles need not make small displacements from the equilibrium point; and the sideband amplitudes need not be small. We have found that the sideband behavior depends sensitively on a phase relationship that exists for a LAW and an upper and lower sideband. When we replace the single particle in each well of the LAW with the more realistic case of many electrons trapped in each well, the essential features of the instability remain the same.

The paper has been organized in the following manner. In Sec. II we review the theory. In Sec. III we present our numerical results, and in Sec. IV we state our conclusions.

II. THEORY

The nonlinear trapped particle state that we wish to study is the one which results from the saturation of the low-density, cold electron beam–plasma instability.[9] It can be shown[10] that the equations that govern the weak, cold beam–plasma interaction are identical to those[11] that describe the weak cold beam–slow wave structure[12] interaction in the weak beam limit. Thus the theory presented below is applicable to both of these systems.

We restrict ourselves to the case in which the resonance condition, Eq. (1), can be satisfied for sidebands that have a large frequency separation, $\Delta\omega$, from the LAW. Namely, we require that $\Delta\omega(1 - v_L/v_g)L/v_L \gg 1$, where L is the length of the plasma and v_g is the group velocity at f_L. When this inequality is satisfied, an electron traveling at velocity v_L is in the plasma long enough to resolve the main wave from the sideband. In the opposite limit the electron transit time is so short that a single electron sees an essentially monochromatic wave. In this case the KDS model is not appropriate, and the modulational theory of DeNeef, Malmberg, and O'Neil[13] is the proper description.

The one-dimensional, many-wave theory of the weak, cold beam–plasma interaction has been given previously,[14] so we give only a brief summary here. The electron beam is assumed to be monoenergetic and the spectrum is assumed to consist of three waves. The interaction between the waves and the beam is governed by three equations—Poisson's equation, Newton's law, and an equation of charge conservation. We define the following scaled parameters:

$$\eta_n = \left(-\frac{\omega_b^2}{\omega_n^2} \frac{1}{(u_0/\omega_n) k_{0n_r}^2 (\partial\epsilon/\partial k)_{\omega_n}} \right)^{1/3}, \tag{2}$$

$$b_n = (1/\eta_n)(u_0 k_{0n_r}/\omega_n - 1), \tag{3}$$

where ω_b and u_0 are the plasma frequency and velocity of the injected beam, ω_n and k_{0n} are the frequency and complex wavenumber of the nth wave, k_{0n_r} is the real part of the wavenumber, and ϵ is the plasma dielectric function in the absence of the beam. Physically, η_n corresponds to the scaled linear growth rate of the nth wave in the case when it is the only wave growing in the system. The fractional difference between the nth wave phase velocity and the injected beam velocity is $b_n\eta_n$. Using these parameters we define the following scaled variables:

$$y = \eta_1(\omega_1/u_0)z, \tag{4}$$

$$\phi_0 = (\omega_1/u_0)z_0, \tag{5}$$

$$\phi_n(y,\phi_0) = \omega_n(z/u_0 - t), \tag{6}$$

$$\frac{dz}{dt} = u_0[1 + \eta_1 q(y,\phi_0)], \tag{7}$$

$$V_n(z,t) = 4\eta_1^2 V_0 A_n(y)\cos[\phi_n(y,\phi_0) - \theta_n(y)]. \tag{8}$$

Here, y and ϕ_0 are independent variables and represent the scaled distance and input electron phase. The subscript 1 corresponds to the large amplitude main wave. In the calculation each electron is assigned a unique value of ϕ_0 ($0 \leqslant \phi_0 < 2\pi$) corresponding to its phase within a wavelength of $2\pi u_0/\omega_1$ at injection. In this Lagrangian approach, then, ϕ_0 is used to specify and keep track of the individual electrons. Beyond the point of injection the computed electron phase is represented by the function $\phi_n(y,\phi_0)$. The scaled velocity of the electron relative to the injected beam velocity is given by $q(y,\phi_0)$, and $A_n(y)$ and $\theta_n(y)$ are the scaled amplitude and phase of the nth wave.

In the weak cold beam formalism, Poisson's equation, Newton's law, and the charge conservation equation are manipulated into a form suitable for calculation on a computer. In terms of the above scaled variables, they are

$$\frac{dA_n}{dy} = -\frac{\omega_n}{\omega_1}\left(\frac{\eta_n}{\eta_1}\right)^3 \int_0^{2\pi l} \frac{d\phi_0}{2\pi l} \frac{\sin(\phi_n - \theta_n)}{1 + \eta_1 q}, \tag{9}$$

$$\frac{d\theta_n}{dy} = \frac{\omega_n}{\omega_1}\left(\frac{\eta_n}{\eta_1}\right)^3 \frac{1}{A_n}\int_0^{2\pi l}\frac{d\phi_0}{2\pi l}\frac{\cos(\phi_n-\theta_n)}{1+\eta_1 q} - \frac{\omega_n}{\omega_1}\frac{\eta_n}{\eta_1}b_n, \tag{10}$$

$$\frac{\partial q}{\partial y} = 2\sum_{n=1}^{3}\frac{\omega_n}{\omega_1}A_1\frac{\sin(\phi_n-\theta_n)}{1+\eta_1 q}, \tag{11}$$

$$\frac{\partial \phi_n}{\partial y} = \frac{(\omega_n/\omega_1)q}{1+\eta_1 q}. \tag{12}$$

The l in the limits of integration is an integer satisfying $2\pi l = \omega_1 T$, where T is the period of the total signal voltage, $\Sigma_{n=1}^{3} V_n(z,t)$ (T is well defined only when the ω_n's are commensurate). From Eqs. (9)–(12) we can derive conservation of momentum,

$$\frac{d}{dy}\left[\sum_{n=1}^{3}\left(\frac{\eta_1}{\eta_n}\right)^3 A_n^2 + \int_0^{2\pi l}\frac{d\phi_0}{2\pi l}q\right] = 0. \tag{13}$$

We integrate Eqs. (9)–(12) numerically. The step size is $\Delta y = 0.01$ and we use 600 electrons in l main wave wavelengths. As a check on the accuracy of the calculation we ensure that Eq. (13) is satisfied; A_1 and q are of order unity, and the discrepancy is always less than 2×10^{-5}.

The Kruer, Dawson, and Sudan approximation essentially consists of replacing the beam with a single particle placed in each well of the LAW. Actually, the replacement we make in our simulation is more realistic than the original KDS calculation since the amplitude and phase variation of the LAW are included, the well is sinusoidal rather than harmonic, the particles need not make small displacements from the equilibrium point, and the sideband amplitudes need not be small.

III. RESULTS

In this section we present our basic findings. We first give the results for the simple case of a single particle placed in the bottom of each well at the beginning of the simulation. Next we consider the case in which the particle is started with a finite displacement away from the bottom of each well. Finally, we consider the realistic case of sideband growth caused by the trapping of a beam from the LAW, that is, many particles in each well.

Before presenting these results, we first show that there exists a well-defined phase relationship among three waves with equally spaced frequencies. From Eqs. (6) and (8), the total electric field to lowest order in η_1 is

$$\begin{aligned}E(z,t) &= 4\eta_1^2\frac{\omega_1 V_0}{u_0}A_1(y)\sin\left[\omega_1\left(\frac{y}{\eta_1\omega_1}-t\right)-\theta_1(y)\right]\\ &+ 4\eta_1^2\frac{\omega_2 V_0}{u_0}A_2(y)\sin\left[\omega_2\left(\frac{y}{\eta_1\omega_1}-t\right)-\theta_2(y)\right]\\ &+ 4\eta_1^2\frac{\omega_3 V_0}{u_0}A_3(y)\sin\left[\omega_3\left(\frac{y}{\eta_1\omega_1}-t\right)-\theta_3(y)\right].\end{aligned} \tag{14}$$

At $y = 0$, we can write this as

$$E(0,t) = (i/2)E_s\{\exp[i\psi_1(t)] + \epsilon_2\exp[i\psi_2(t)] + \epsilon_3\exp[i\psi_3(t)] - \text{c.c.}\}, \tag{15}$$

where

$$E_s = 4\eta_1^2(\omega_1 V_0/u_0)A_1(0), \tag{16}$$

$$\epsilon_2 = (\omega_2/\omega_1)[A_2(0)/A_1(0)], \tag{17}$$

$$\epsilon_3 = (\omega_3/\omega_1)[A_3(0)/A_1(0)], \tag{18}$$

and

$$\psi_1(t) = \omega_1 t + \theta_1(0), \tag{19}$$

$$\psi_2(t) = (\omega_1+\Delta\omega)t + \theta_2(0), \tag{20}$$

$$\psi_3(t) = (\omega_1-\Delta\omega)t + \theta_3(0). \tag{21}$$

We see that the quantity

$$\Theta_0 = \psi_2(t) + \psi_3(t) - 2\psi_1(t) = \theta_2(0) + \theta_3(0) - 2\theta_1(0) \tag{22}$$

is time independent but depends on the values of the initial phases. It is a characteristic of the signal and cannot be removed by a time translation. The quantity Θ_0 defines a phase relationship among the three waves that is invariant in time.

We can also write Eq. (15) as

$$E(0,t) = (i/2)\{c(t)\exp[i(\omega t + \Phi(t))] - \text{c.c.}\}, \tag{23}$$

and when $\epsilon_0 = \epsilon_2 = \epsilon_3 \ll 1$,

$$\begin{aligned}c(t) &= E_s[1 + 2\epsilon_0\cos\Delta\omega t\cos(\Theta_0/2)],\\ \Phi(t) &= \gamma + 2\epsilon_0\cos\Delta\omega t\sin(\Theta_0/2).\end{aligned} \tag{24}$$

Thus, when $\Theta_0/2 = 0$, we can consider the three waves as an amplitude modulated wave

$$E_{\text{AM}} = E_s(1 + 2\epsilon_0\cos\Delta\omega t)\cos(\omega_0 t + \gamma), \tag{25}$$

and when $\Theta_0/2 = \pi/2$, we can consider the three waves as a frequency modulated wave

$$E_{\text{FM}} = E_s\cos(\omega_0 t + 2\epsilon_0\cos\Delta\omega t + \gamma). \tag{26}$$

We can generalize the invariant phase to $y \neq 0$. Let us rewrite Eq. (15) as

$$E = (i/2)E_s(y)\{\exp[i\psi_1(y,t)] + \epsilon_2(y)\times\exp[i\psi_2(y,t)] + \epsilon_3(y)\exp[i\psi_3(y,t)] - \text{c.c.}\}, \tag{27}$$

where

$$\psi_n(y,t) = -\omega_n(y/\eta_1\omega_1 - t) + \theta_n(y) \tag{28}$$

and we form in analogy with Eq. (22),

$$\Theta(y) = \psi_2(y,t) + \psi_3(y,t) - 2\psi_1(y,t) = \theta_2(y) + \theta_3(y) - 2\theta_1(y). \tag{29}$$

This quantity may be interpreted as the spatial variation of the sum of two phases: the upper sideband phase relative to the main wave phase plus the lower sideband phase relative to the main wave phase. For the situation depicted in Figs. 1(b) and 1(c) this quantity is zero.

A. Single particle case

We now present the results for the sideband behavior in the simple case of a single particle placed in the bottom of each well. The velocity of the particle relative to the well is zero at the beginning. Figure 2(a) is a plot of the logarithm of the electric field amplitude, $20\log[2(\omega_n/\omega_1)A_n]$, versus axial distance y. The solid curve corresponds to the LAW; the dashed and dotted curves correspond to the upper and

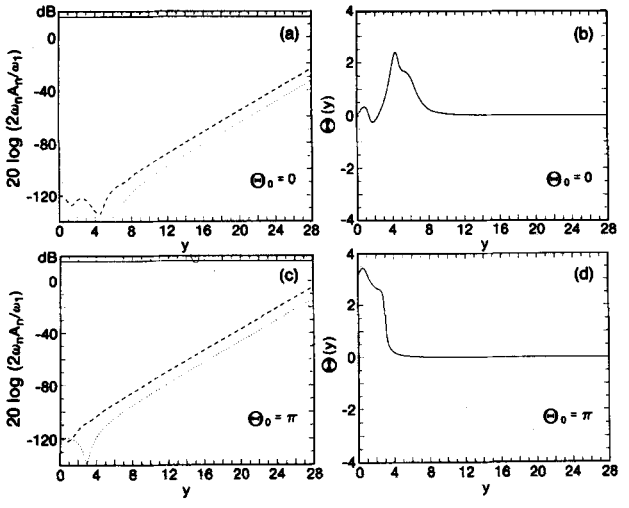

FIG. 2. Simulation results for a particle placed at the bottom of each well. (a) Wave electric field of the LAW (solid line), upper sideband (dashed line), and lower sideband (dotted line) versus distance for $\Theta_0 = 0$. (b) Invariant phase versus distance for $\Theta_0 = 0$. (c) Wave electric field versus distance for $\Theta_0 = \pi$. (d) Invariant phase versus distance for $\Theta_0 = \pi$. $\eta_1 = \eta_2 = \eta_3 = 0.01$; $b_1 = -0.33$, $b_2 = 2.10$, $b_3 = -2.94$; $A_1(0) = 3.0$, $A_2(0) = 4.286\times10^{-6}$, $A_3(0) = 6.00\times10^{-6}$; $\omega_{r_2} = \frac{7}{6}$, $\omega_{r_3} = \frac{5}{6}$.

lower sidebands, respectively. At $y = 0$, the waves are started in the form of a pure amplitude modulation of the LAW ($\Theta_0 = 0$). The phase velocities of the sidebands have been chosen to maximize the sideband growth rates. The sidebands are seen to grow smoothly by approximately 9 dB. The upper and lower sidebands behave quite differently in the initial region, $y < 12$. Beyond $y \cong 12$ they grow at the same asymptotic growth rate until they reach approximately the same amplitude as the LAW and detrap the particle. In Fig. 2(b) we plot the invariant phase, $\Theta(y)$, vs y. It exhibits some variation for $y < 10$ but beyond $y \cong 10$ it remains near zero. Figure 2(c) shows a plot of $20\log[2(\omega_n/\omega_1)A_n]$ vs y for the case where the waves are started in the form of a pure frequency modulation of the LAW ($\Theta_0 = \pi$). Again the upper and lower sidebands behave quite differently from one another in the region $y < 8$. Beyond this point they grow at the same asymptotic growth rate as in the case for $\Theta_0 = 0$ [Fig. 2(a)]. However, by $y = 28$ the upper and lower sideband levels are 20 dB higher than the corresponding levels in Fig. 2(a). We see that the value of Θ_0 strongly affects the sideband growth rates near the beginning of the instability, and that although the asymptotic growth rate does not depend on Θ_0, the amplitudes of the sidebands in the asymptotic growth region do depend on Θ_0. In Fig. 2(d) we show the corresponding plot of $\Theta(y)$ vs y. In this case $\Theta(y)$ is seen to evolve from $\Theta_0 = \pi$ to an asymptotic value, $\Theta_{\text{asym}} = 0$. In the initial region $y < 10$, the sidebands adjust their phases so as to attain the asymptotic value $\Theta_{\text{asym}} = 0$. The ratio of the sideband amplitudes in the asymptotic growth region is given by the KDS theory. Neglecting terms of order η_1,

$$|E_2/E_3|_{\text{asym}} = |\omega_{r_2}/(\omega_{r_2} - 2)|^3, \tag{30}$$

where $\omega_{r_2} = \omega_2/\omega_1$, E_2 and ω_2 are the electric field amplitudes and angular frequency of the upper sideband, respectively, and E_3 and ω_3 are the corresponding quantities for the lower sideband. For the parameters of Fig. 2, the asymptotic ratio of the sideband electric field amplitudes is 8.77 dB. The simulation agrees well with this expression. In Figs. 2(a) and 2(c) the asymptotic ratio is seen to be 9 dB. In the limit $\omega_r \to 1$, we would have $|E_2/E_3|_{\text{asym}} \to 1$ and $\Theta_{\text{asym}} = 0$. Therefore, in this limit the LAW and the sidebands are equivalent to an amplitude modulation of the LAW. In general, for sufficiently small, equally spaced sidebands one can represent a launched signal at $y = 0$ as a mixture of amplitude and frequency modulation. The system evolves in such a way that in the asymptotic growth region the LAW is purely amplitude modulated. As seen in Fig. 2, even when $|E_2/E_3| \neq 1$ and thus the modulation is not quite pure amplitude modulation in the asymptotic growth region, we still have $\Theta_{\text{asym}} = 0$, corresponding to the value associated with amplitude modulation. It is interesting to note that although the sidebands adjust their wave phases so that $\Theta_{\text{asym}} = 0$, at $y = 28$ the amplitudes of the sidebands launched with $\Theta_0 = \pi$ are much higher than the levels of those launched with $\Theta_0 = 0$.

We have checked that the growth rates and real wavenumber shifts in the asymptotic growth region agree with those given by the KDS analytic theory. In Fig. 3 we show the scaled growth rate, $v_L\,\delta k_i/\eta_1\omega_1$, and the scaled real wavenumber shift, $v_L\,\delta k_r/\eta_1\omega_1$, as a function of the scaled phase velocity $(u_0/v - 1)/\eta_1$. Here δk_i and δk_r are the growth rate and real nonlinear wavenumber shift, respectively, and v is the phase velocity. The dots represent the result of the simulation and the line is the result of the KDS analytic theory. The dashed lines indicate the scaled phase velocities at which Eq. (1) is satisfied. The agreement is seen to be good.

The equations we use to generate Fig. 2 are Eqs. (9)–(12) simplified by following only one particle in each well of the LAW. A complication arises when Eq. (10) is simplified to the single particle case. For the LAW at $y = 0$, we have

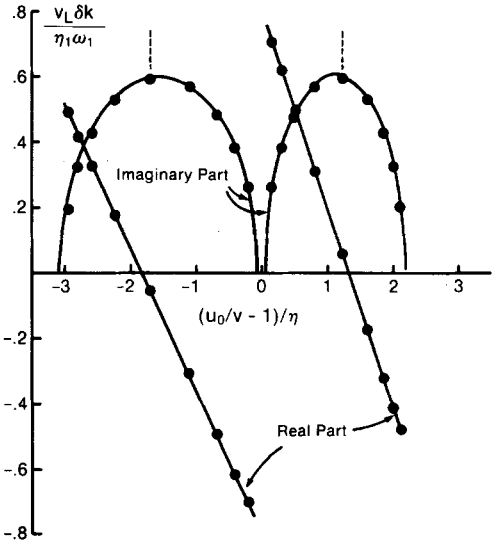

FIG. 3. Growth rate and real wavenumber shift versus scaled phase velocity for simulation (dots) and for analytic theory (lines). $A_1(0) = 1.0$, $A_2(0) = 1.0\times10^{-6}$, $A_3(0) = 1.0\times10^{-6}$. All other parameters are the same as in Fig. 2.

$$\left(\frac{d\theta_1}{dy}\right)_0 = \frac{1}{A_1(0)}\cos(\phi_1 - \theta_1) - b_1, \tag{31}$$

where b_1 is an input parameter that expresses the difference between the particle velocity and the LAW phase velocity in the absence of the particles. The most natural choice for b_1 is $b_1 = 0$. However, this choice causes a large phase shift to be initiated at $y = 0$. Since $A_1(0)$ is of order unity, and since $\phi_1 = \theta_1 = \pi$ for a particle placed at the bottom of the well, the right-hand side of Eq. (31) is of order unity. Physically, this phase shift is a result of a change in the wave dispersion caused by the presence of the particles. This large phase shift of the LAW causes the particle to oscillate with a large amplitude and thereby causes large trapping oscillations. We avoid this effect by choosing $b_1 = -1/A_1(0)$. With this choice no large phase shifts occur, no significant trapping oscillations occur, and there is no essential deviation from the KDS theory.

Perhaps a more natural way to deal with this problem of large phase shifts is to choose $b_1 = 0$ and place the particle at $\phi_1 - \theta_1 = \pi/2$ or $3\pi/2$. Again the right-hand side of Eq. (31) is zero, but the problem is complicated by introducing a large initial oscillation amplitude of the particle. However, this is quite sensible physically, since in the many-particle case the beam electrons are not trapped at the very bottom of the well. Instead, they execute rather large phase displacements away from the equilibrium point at the bottom of the well.

In Fig. 4 we exhibit the same types of plots as in Fig. 2 but with the particle placed at $\phi_1 - \Theta_1 = 3\pi/2$ at $y = 0$. The phase velocities of the sidebands have been chosen to maximize the sideband growth rates, and the particle velocity relative to the LAW phase velocity is zero at $y = 0$. Figure 4(a) is a plot of 20 log $(2\omega_n A_n/\omega)$ vs y for $\Theta_0 = 0$. The LAW is seen to execute large trapping oscillations as expected. In addition, both the upper and lower sidebands are seen to execute oscillations at twice the bounce wavenumber. The sideband growth rate is much lower than that shown in Fig. 2(a). In Fig. 4(b) we show the corresponding plot of $\Theta(y)$ vs y. After undergoing a large oscillation in the region $y < 10$, the invariant phase oscillates about the amplitude modulation value, $\Theta_{\text{asym}} = 0$. Figure 4(c) shows a plot of 20 $\times$log $A(y)$ vs y for the case of $\Theta_0 = \pi$. Again we see large trapping oscillations of the main wave and oscillations in the sideband. Just as in Figs. 2(a) and 2(c), we see that the level of the upper sideband is on average higher than that of the lower sideband. In addition, we see that at $y = 32$, the levels of both upper and lower sidebands are 10 dB higher for $\Theta_0 = \pi$ [Fig. 4(c)] than for $\Theta_0 = 0$ [Fig. 4(a)]. In Fig. 4(d) we show the corresponding plot of $\Theta(y)$ vs y. Here, $\Theta(y)$ is seen to shift from $\Theta_0 = \pi$ toward $\Theta(y) = 2\pi$ and then to oscillate about this value. Since the invariant phase is only uniquely specified up to integer multiples of 2π, again we see that $\Theta(y)$ oscillates about the value corresponding to amplitude modulation. In summary, starting the particle out at a finite oscillation amplitude at $y = 0$ decreases the sideband growth rate and introduces an oscillatory behavior in both the wave amplitude and the invariant phase.

B. Many-particle case

In Fig. 5 we show the evolution of the electric field and the invariant phase for the many-particle case. The sideband phase velocities have again been chosen to maximize the growth rate. At $y = 0$, the LAW is launched in the presence of a uniform density beam. The beam is then immediately trapped by the LAW. The LAW is launched at a level roughly three times the saturation level and the beam is deeply trapped. The beam particles oscillate near the bottom of the well and the LAW exhibits little amplitude variation. In Figs. 5(a) and 5(c) we display the evolution of the electric field for the cases where the waves are launched with $\Theta_0 = 0$ and $\Theta_0 = \pi$. Although the LAW is of nearly constant ampli-

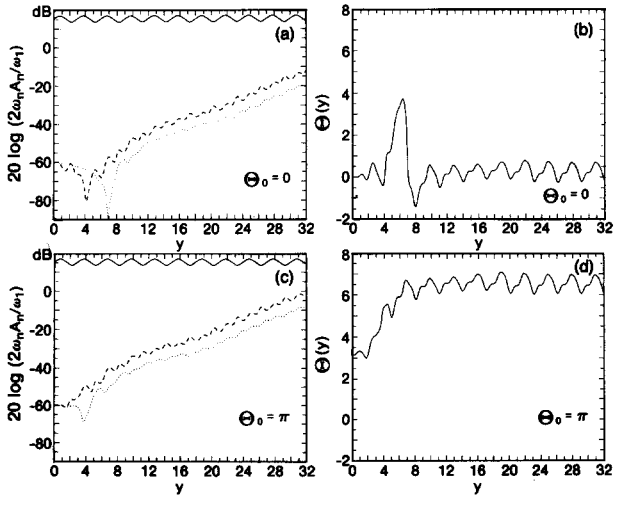

FIG. 4. Simulation results for a particle placed at a finite amplitude in the well. (a) Wave electric field of the LAW (solid line), upper sideband (dashed line), and lower sideband (dotted line) versus distance for $\Theta = 0$. (b) Invariant phase versus distance for $\Theta_0 = 0$. (c) Wave electric field versus distance for $\Theta_0 = \pi$. (d) Invariant phase versus distance for $\Theta_0 = \pi$. $b_1 = 0$, $b_2 = 1.70$, $b_3 = -2.38$; $A_1(0) = 3.0$, $A_2(0) = 4.286 \times 10^{-4}$, $A_3(0) = 6.00 \times 10^{-4}$. All other parameters are the same as in Fig. 2.

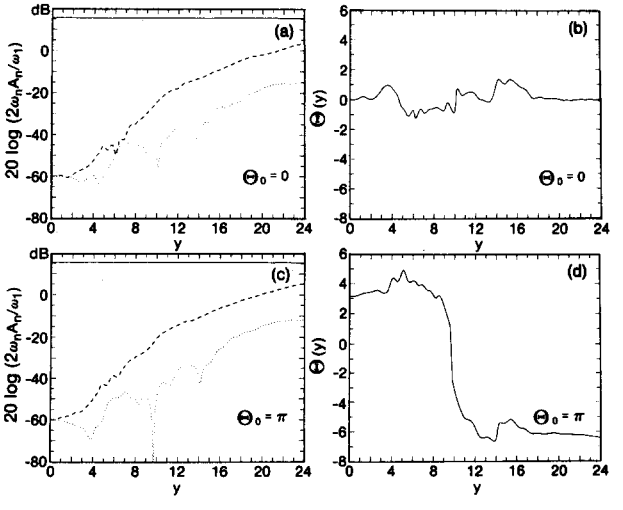

FIG. 5. Simulation results for beam electrons trapped by the LAW. (a) Wave electric field of the LAW (solid line), upper sideband (dashed line), and lower sideband (dotted line) versus distance for $\Theta_0 = 0$. (b) Invariant phase versus distance for $\Theta_0 = 0$. (c) Wave electric field versus distance for $\Theta_0 = \pi$. (d) Invariant phase versus distance for $\Theta_0 = \pi$. $b_1 = 0$, $b_2 = 2.2$, $b_3 = -3.080$. All other parameters are the same as in Fig. 4.

tude, similar to the bottom of the well case (Fig. 2), the sidebands undergo large oscillations as they grow, similar to the finite oscillation amplitude case (Fig. 4). The sideband growth rate is larger than that for the finite oscillation amplitude case but smaller than that for the bottom of the well case. As in both cases, the level of the upper sideband is on average higher than that of the lower sideband. Also, as in both cases, Figs. 5(b) and 5(d) show the invariant phase for $\Theta_0 = 0$ and π evolving to the amplitude modulation value (0 and, equivalently, -2π) asymptotically. Again we see that the value of Θ_0 affects the sideband behavior, especially near the beginning of the instability.

IV. CONCLUSION

The essential features of the sideband instability that occurs when a large amplitude wave traps an electron beam are well described by a simple model in which a single particle oscillates in each well of the LAW. Both upper and lower sidebands are unstable and their behavior is dependent on an invariant phase relationship that exists between the two sidebands and the LAW. For sufficiently small sidebands, an upper and lower sideband launched at equal frequency separation from a LAW are equivalent to a mixture of frequency and amplitude modulation of the LAW. The value of the invariant phase expresses this mixture. As the interaction proceeds, the phases of the sidebands adjust so that in the asymptotic growth region the value of the invariant phase corresponds to that associated with amplitude modulation.

ACKNOWLEDGMENTS

We wish to thank Professor Roy Gould, Professor Norman Kroll, and Professor Thomas O'Neil for many valuable conversations.

This material is based upon work supported by the National Science Foundation under Grant No. PHY80-90326 and No. PHY83-06077.

[1] C. B. Wharton, J. H. Malmberg, and T. M. O'Neil, Phys. Fluids **11**, 1761 (1968).
[2] R. N. Franklin, S. M. Hamberger, H. Ikezi, G. Campis, and G. S. Smith, Phys. Rev. Lett. **28**, 1114 (1972).
[3] J. H. A. van Wakeren and H. J. Hopman, Phys. Rev. Lett. **28**, 295 (1972).
[4] G. Van Hoven and G. Jahns, Phys. Fluids **18**, 80 (1975).
[5] T. P. Starke and J. H. Malmberg, Phys. Fluids **21**, 2242 (1978).
[6] W. L. Kruer, J. M. Dawson, and R. N. Sudan, Phys. Rev. Lett. **23**, 838 (1969).
[7] G. J. Morales, Phys. Fluids **23**, 2472 (1980).
[8] A. L. Brinca, J. Plasma Phys. **7**, 382 (1972).
[9] T. M. O'Neil, J. H. Winfrey, and J. H. Malmberg, Phys. Fluids **14**, 1204 (1971).
[10] S. I. Tsunoda and J. H. Malmberg, Phys. Fluids **27**, 2557 (1984).
[11] A. Nordsieck, Proc. IRE **41**, 630 (1953).
[12] J. R. Pierce, *Traveling Wave Tubes* (Van Nostrand, New York, 1950).
[13] C. P. DeNeef, J. H. Malmberg, and T. M. O'Neil, Phys. Rev. Lett. **30**, 1032 (1973).
[14] M. K. Scherba and J. E. Rowe, IEEE Trans. Electron Devices **ED-18**, 11 (1971).